



**HAL**  
open science

# A Simple Analytical Approximation to evaluate Noise Levels and Maximum Coupling Frequencies During DPI Simulations on BMS IC

Badr Guendouz, Philippe Perruchoud, Kamel Abouda, Alexandre Boyer,  
Sonia Ben Dhia

► **To cite this version:**

Badr Guendouz, Philippe Perruchoud, Kamel Abouda, Alexandre Boyer, Sonia Ben Dhia. A Simple Analytical Approximation to evaluate Noise Levels and Maximum Coupling Frequencies During DPI Simulations on BMS IC. Asia Pacific International Conference on EMC (APEMC) 2022, Sep 2022, Beijing, China. 10.1109/APEMC53576.2022.9888479 . hal-03773319

**HAL Id: hal-03773319**

**<https://hal.laas.fr/hal-03773319>**

Submitted on 9 Sep 2022

**HAL** is a multi-disciplinary open access archive for the deposit and dissemination of scientific research documents, whether they are published or not. The documents may come from teaching and research institutions in France or abroad, or from public or private research centers.

L'archive ouverte pluridisciplinaire **HAL**, est destinée au dépôt et à la diffusion de documents scientifiques de niveau recherche, publiés ou non, émanant des établissements d'enseignement et de recherche français ou étrangers, des laboratoires publics ou privés.

# A Simple Analytical Approximation to evaluate Noise Levels and Maximum Coupling Frequencies During DPI Simulations on BMS IC

Badr Guendouz<sup>(1)(2)</sup>, Philippe Perruchoud<sup>(1)</sup>, Kamel Abouda<sup>(1)</sup>

(1) BMS/EMC TEAMS  
NXP Semiconductors  
Toulouse, France

Alexandre Boyer<sup>(2)</sup>, Sonia Ben Dhia<sup>(2)</sup>

(2) LAAS-CNRS  
Univ. de Toulouse, INSA, UPS, LAAS  
Toulouse, France

**Abstract**— Many works [2][3] make use of high frequency battery models and Printed Circuit Board (PCB) models for EMC emission characterization. This work proposes those models in addition to a Battery Management System (BMS) impedance to show the effect on the noise received by the BMS under Direct Power Injection (DPI) simulations with different external components configurations. Furthermore, in order to ease some of the first design stages of the BMS and its external components, a straightforward analytical model to estimate the noise levels and its maximum coupling frequencies during DPI simulations is also elaborated and validated by simulations.

**Keywords**—Battery Management System; PCB; Battery; High Frequency; DPI; Resonance; Noise levels.

## I. INTRODUCTION

Lithium Ion (Li-Ion) batteries as well as BMS [1] have been subject to extensive research to pave the way for the new generation of electric vehicles (EV) and hybrid electric vehicles (HEV). One major aspect of development, for example, is the characterization of the conducted EMI coming from the drive inverter [2] which is one of the noise sources that can act as an aggressor to the BMS IC. In this noise path, the high frequency (HF) impedance of the battery, PCB traces, and BMS impedance highly contribute to the correct assessment of the incoming noise spectrum. While a number of articles [2][3] deal with the later point, this article investigates the effect of those components during EMC simulations of the BMS integrated circuit (IC). Indeed, during the design flow of the BMS IC, the simulation of standard EMC measurement tests such as direct power injection (DPI) [6] is performed along the way to evaluate the immunity of the IC and perform design changes and optimizations. Therefore, choosing the right model for either the battery or the PCB traces plays a major role in the noise injection levels. More importantly, the configuration by which some of the external components are connected directly alters the noise coupling frequencies, for example; whether some electrostatic discharge (ESD) protection capacitors are connected in a differential way or to ground. Therefore, having an on-hand simple predictive model of the main noise coupling frequencies and injection levels in the early design stages can be vital for both properly characterizing the immunity levels of the BMS IC and understanding different design choices for the BMS IC external components such as filters, protection capacitor, etc. The goal of

this article is to provide a simple modeling approach of the BMS itself and its environment during DPI simulations as well as a predictive analytical model of injected noise levels at the main coupling frequencies. This paper is organized as follows; First, some basic notions of the BMS IC front end will be given. Secondly, the considered models for each of the battery, PCB traces, BMS IC and DPI injection will be presented. Thirdly, the effect of using an HF model for the battery instead of an ideal voltage source for different ESD capacitors configurations by DPI simulation will be shown. Lastly, an analytic approach to predict the main noise coupling frequencies while performing DPI will be elaborated.

## II. TYPICAL BMS IC FRONT END

The main purpose of a BMS is to ensure the proper and safe operation of the battery especially with Li-Ion chemistry-based batteries which have to operate under a certain temperature and voltage range. Some of the main functions of a BMS are then to perform accurate cell voltage measurement and passive cell balancing [1] to prevent cell degradation and enable optimum power extraction from the battery pack. Fig. 1 shows a high level diagram of the BMS front-end and surrounding external environment, where,  $S_i$  are the balancing switches,  $C_d$  are an ESD protection capacitor and  $R_b$  the balancing resistor.

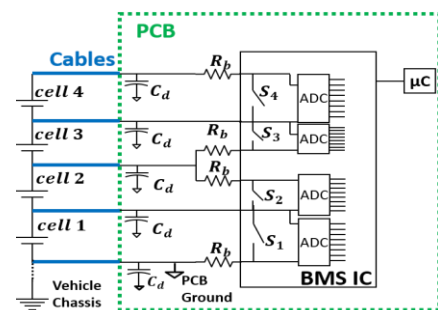


Fig. 1. Typical high level view of a BMS IC front end

## III. MODELING OF THE BMS ‘CHAIN’ APPLICATION

The goal of this section is to elaborate on the battery, PCB and BMS IC models which are crucial to run reliable DPI simulations on one hand but also to pave the way to a simple analytical approach to predicting the injection levels as well as the main noise coupling frequencies.

### A. High Frequency Battery Model (HFBM)

An HFBM was developed internally at NXP semiconductors which describes the HF impedance of a 400Wh cell from a battery pack currently in production, in the following range [150 KHz; 100 MHz]. Fig. 2 displays the used HFBM along with the values of the main components.

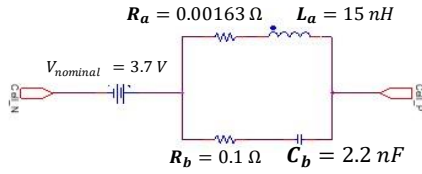


Fig. 2. Electrical model of the HF impedance of the battery

In the following figure, the measured impedance of the battery pack is plotted as a function of frequency.

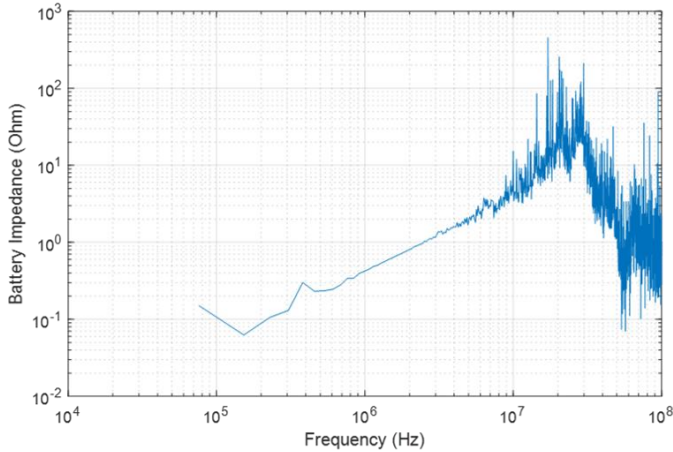


Fig. 3. Measured impedance profile of the battery from 150 KHz to 100 MHz.

### B. BMS IC Model

In order to simplify this paper's approach, the main contributor to the impedance presented by the BMS IC is considered to be the cell balancing switch. Indeed, these switches are designed to have a large area to have minimum heat dissipation in the IC during passive cell balancing, and thus present a relatively considerable equivalent capacitor value. By simulating the parasitic capacitances of an existing switch design, an ideal capacitor  $C_L$  of 30 pF was chosen as a representation.

### C. PCB Traces and DPI Model

In Fig. 1, the PCB is modeled depending on the considered length. Considering that the range of interest is [150 KHz; 100 MHz] and knowing that the maximum length belongs to the battery cables (in blue in Fig. 1) which is 20 cm, a simple lumped model could be used to model the traces. With the presence of capacitor  $C_d$  (47 nF) and  $R_b$  with a value of 15  $\Omega$ , the capacitive and resistive effects of the cable and traces models is neglected. Thus, only inductors are used to model the cables as well as the sectioned traces with values depending on the length.  $L_0$  in Fig. 4 models the battery cable (200 nH) while  $L_1$  models different sections of the PCB traces. In addition, a realistic model of capacitor  $C_d$  is used as it includes its inductive and

resistive behavior. When it comes to DPI, it is implemented in common mode way where 30 dBm is coupled to the PCB traces through  $R_i$  and  $C_i$  (6.8nF) as the standards require. Based on the setup of Fig. 4, four configurations will be presented to compare the corresponding injection levels:

- Config A: ideal voltage source ( $V_{DC}$ ) with capacitors  $C_d$  connected to ground.
- Config B: HFBM  $V_{HFBM}$  with capacitors  $C_d$  connected to ground.
- Config C:  $V_{DC}$  with capacitors  $C_d$  differentially connected.
- Config D: HFBM  $V_{HFBM}$  with capacitors  $C_d$  differentially connected.

Finally, in order to extract the peak-to-peak differential voltage across the load capacitors, transient simulations were performed in SPICE environment where:

- The simulation was given enough period for the signals to settle (above 500 periods) before extracting any data.
- The peak-to-peak values for each injected frequency were extracted as an average on the data of the last 50 periods of the signal.
- Lastly, a sufficient numbers of points per decades were taken in the range of [150 KHz; 100 MHz] (500 pts/decades).

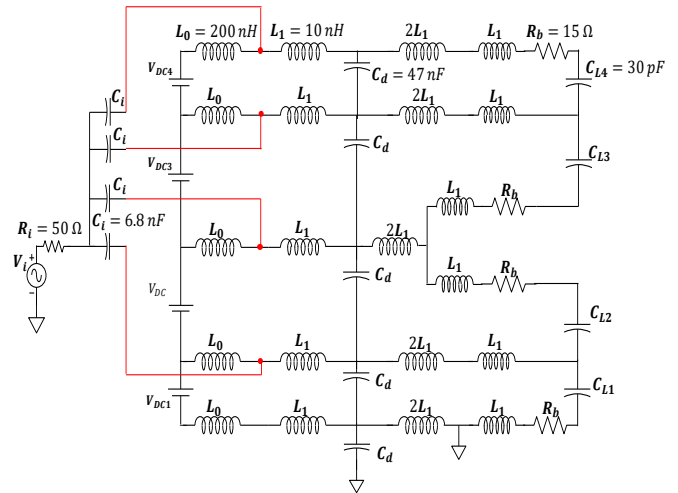


Fig. 4. Modeling of the PCB traces and DPI CM injection for config C as an example.

In the following section, the simulation results will be shown and an interpretation of the main comparison aspects will be elaborated.

## IV. DPI SIMULATIONS ON THE BMS CHAIN MODEL

In this section, the comparison will be elaborated between config A and config B on one hand, and between config C and config D on another hand in terms of the peak-to-peak differential voltage generated across the load capacitors CL1, CL2, CL3 and CL4. This value will be denoted as  $V_{pk2pk}(CLi)$ .

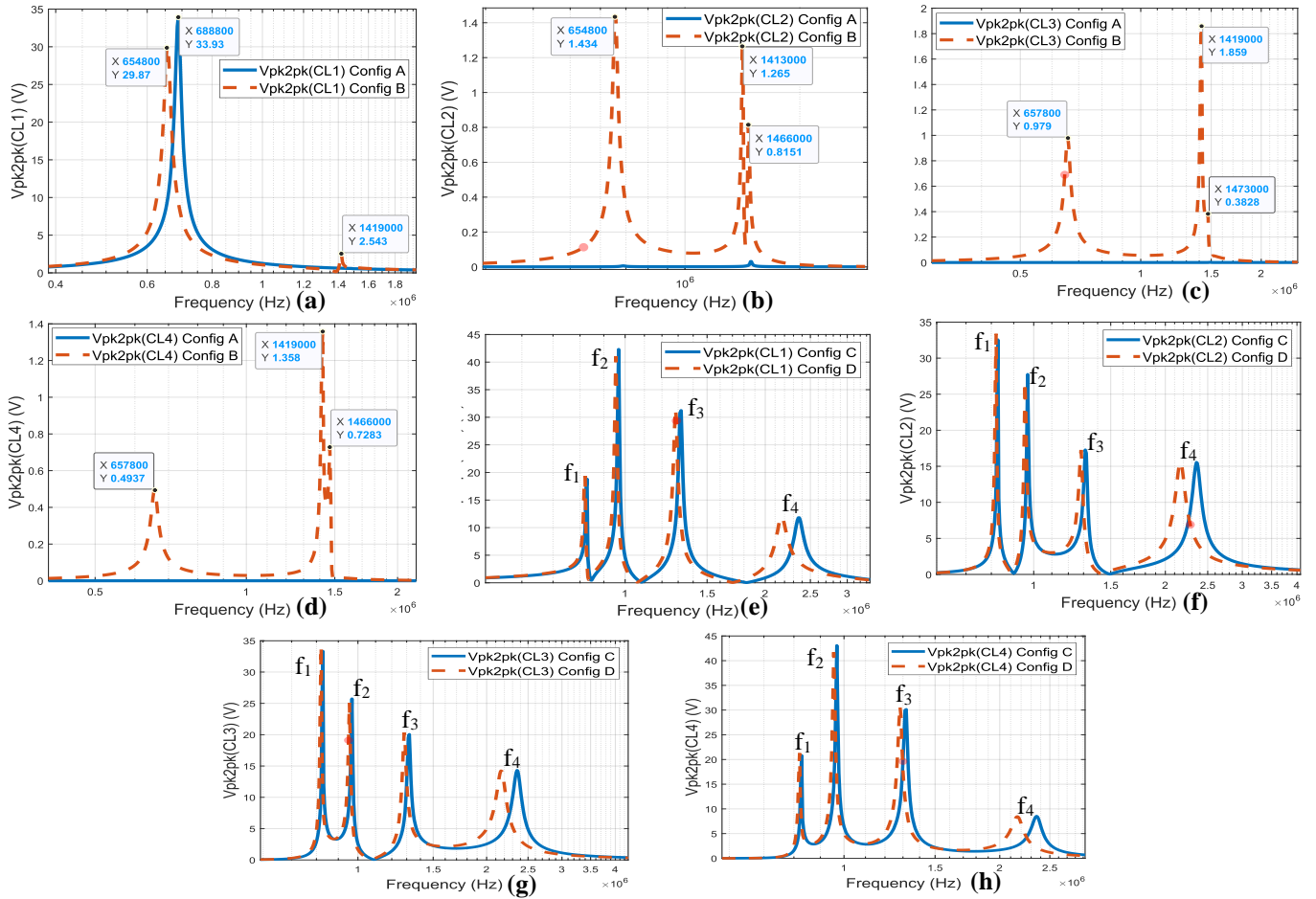


Fig. 5.  $V_{pk2pk}(C_{Li})$  simulation results as a function of the injected frequency and comparing Config A with B and Config C with D. In the exception of the shown frequency range, the two curves of each graph fit together.

#### A. Config A Vs Config B

From Fig. 5a,b,c,d, it can be seen that with the HFBM more resonance frequencies are included, thus more frequencies on which the BMS IC could be characterized and optimized. Furthermore, it can also be seen that as one goes from  $C_{L2}$  to  $C_{L4}$  in config B, no noise is coupled onto the BMS IC compared to considerable injection in config A. This can be explained by the fact that in config A,  $V_{DC}$  is simply a short and since the injection is performed in a CM way and  $C_d$  is connected to ground, the PCB traces are perfectly symmetrical above the first battery cell stage. Thus, it leads to the absence of any CM to differential mode conversion.

#### B. Config C Vs Config D

From Fig. 5e,f,g,h, it can be seen that either with config C or D, the number of resonance frequencies is the same with the main effect being a slight shift of those frequencies. In other words, the effect of including the HFBM with  $C_d$  differentially connected is not as major as in the case of the previous section. This can be explained by the fact that the dominant coupling between the PCB traces is through capacitors  $C_d$  due to its relatively larger value (47nF). Additionally, it can be noticed from Fig. 5e,f,g,h with respect to Fig. 5a,b,c,d that connecting the ESD protection capacitor in a differential way leads to an

increase of resonance frequencies. Furthermore, these coupled oscillations portray a far greater level of induced peak-to-peak voltage on the BMS IC side. More importantly, connecting the capacitor  $C_d$  differentially does imply a lower price as it would be rated for low voltages, however this comes with an increase in noise coupling frequencies as well as its level. On the other hand, connecting the capacitors with ground implies a higher price as it would be rated for high voltages, however, symmetry of the PCB traces in terms of impedance is gained.

In next section, a simple analytical model is proposed for the case of Config C.

### V. ANALYTICAL MODEL OF NOISE COUPLING FREQUENCIES AND INJECTION LEVELS

In order to approach a simple analytical model, some considerations have to be elaborated in the case of Config C (Fig. 4). First, in the context of config C and due to the high ratio between  $C_d$  and  $C_L$ , the effect of the BMS IC could be neglected. Secondly, since the ideal voltage source doesn't present any sort of impedance, it could be considered as a short for AC calculations. Fig. 6 illustrates the model. Furthermore, in order

to ease the approach, a differential DPI injection setup on the up most PCB trace is considered as shown in Fig. 6a.

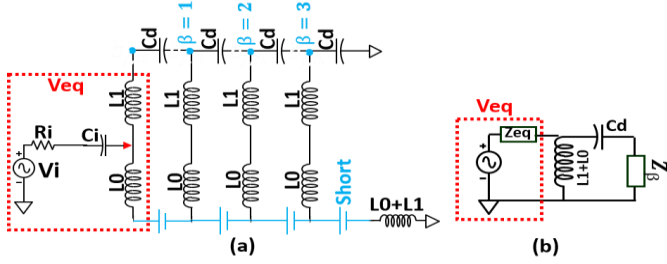


Fig. 6. Simplification of PCB model from Config C. (a) removal of  $C_L$  and  $R_b$ . (b) simplified model using  $Z_\beta$

From Fig. 6a, the PCB traces model now is a C-L ladder network with an input  $V_{eq}$ . The considered outputs in this case are the differential voltages across capacitors  $C_d$ . Based on [4], the following equation gives a first simple approximation to the injection levels:

$$V(C_d) = \frac{\sum_{j=0}^{n-\beta+1} c_{j,n-\beta+1} \left( \frac{1}{s^2(L_0+L_1)C_d} \right)^{j+1}}{\sum_{j=0}^n b_{j,n} \left( \frac{1}{s^2(L_0+L_1)C_d} \right)^j} V_{eq} \quad (1)$$

Where  $C_{j,n-\beta+1}$  and  $b_{j,n}$  are a function of the binomial coefficients [5] and  $\beta$  is the node of interest (Fig. 6a). More interestingly, in order to prove (1), a recursive formula of the impedance seen from any node  $\beta$  to the right between different nodes has to be elaborated. Such an impedance is written as follows [5]:

$$Z_\beta(s) = \frac{\sum_{j=0}^{n-\beta} b_{n-\beta,j} \left( \frac{1}{s^2(L_0+L_1)C_d} \right)^j}{\sum_{j=0}^{n-\beta+1} c_{n-\beta+1,j} \left( \frac{1}{s^2(L_0+L_1)C_d} \right)^{j+1}} \quad (2)$$

Using (2), the PCB traces in Fig. 6a can be simplified as in Fig. 6b when  $\beta=1$ . From Fig. 6b, maximum noise coupling occurs when the impedance reaches a maximal value. Under this condition, the frequencies for which  $Z_\beta$  is maximum. Based on [4], the roots of the denominator of (2). can be written as the following for  $\beta=1$ :

$$f_{N_{cell}}^{(i)} = \frac{1}{4\pi\sqrt{(L_0+L_1)C_d} \sin\left(\frac{i}{2(N_{cell}-\beta+2)}\pi\right)} \quad (3)$$

Where  $N_{cells}$  is the number of cells in the pack and 'i' is the index of the resonance frequency which is included in  $[1; N_{cells}]$ . In order to validate the previous equation, the four resonance frequencies were calculated and compared with their respective simulated values from Fig. 5e,f,g,h (under Config C).

TABLE 1. Calculated and simulated resonance frequencies.

	Config C Simulation	Equation (3)
$f_1$	826.116 kHz	842 kHz
$f_2$	968.481 kHz	990 kHz
$f_3$	1.319 MHz	1.36 MHz
$f_4$	2.366 MHz	2.59 MHz

From Table.1, the simulated resonance frequencies ( with the full PCB traces model) are considerably close to the calculated values. This indeed confirms, to some extent, the set of considerations that were elaborated in the beginning of this section. Therefore, one could directly predict the set of maximum noise coupling frequencies if some capacitors are to be connected differentially between the PCB traces.

## VI. CONCLUSION

Finally, this work has presented some predictive results when it comes to design choices of the BMS IC external components under DPI simulations. Furthermore, a straightforward calculation model has also been presented to easily predict the injection levels as well as the maximum noise coupling frequencies. Future work will focus on validating the presented results by measurements but also on considering the analytical model for some different injection setup or even different tests (e.g. BCI). Additionally, future work will also evaluate having nonlinear components on the BMS IC side such as ESD structures and their effect on noise coupling, perhaps even deducing design rules on such structures to minimize noise coupling.

## VII. REFERENCES

- [1] Andrea, D. Battery management systems for large Lithium-Ion Battery Packs. norwood: Artech house, 2010.
- [2] Zaatari, M. T. High Frequency Battery Impedance Measurements for EMI Prediction. EMC, August 2013 , 763-767. doi:10.1109/IEMC.2013.6670512
- [3] M. Reuter, S. T. Influence of a Traction Battery's Input Impedance on Conducted Emissions of an Automotive HV Inverter. International Symposium on Electromagnetic Compatibility (EMC Europe 2013) (pp. 2-6). Brugge: IEEE.
- [4] Giulio Antonini, G. F. A New Approach for Closed-Form Transient Analysis of Multiconductor Transmission Lines. IEEE TRANSACTIONS ON ELECTROMAGNETIC COMPATIBILITY, VOL. 46, NO. 4, 2004 ,523-543.
- [5] M. Faccio, G. F. A new fast method for ladder networks characterization . IEEE Transactions on circuits and systems, VOL.38, NO. 11, 1991, 1377-1382.
- [6] IEC 62132-4 – edition 1.0: Integrated circuits - Measurement of electromagnetic immunity - Part 4: Direct RF power injection method, 2006-02-21.